Research Article

Comparative assessment of methylene blue biosorption using coffee husks and corn cobs: towards the elaboration of a lignocellulosic-based amperometric sensor

Evangeline Njanja[1] · Serge Foukmeniok Mbokou[1,2,3] · Maxime Pontie[2,3] · Mouna Nacef[4] · Ignas Kenfack Tonle[1]

Abstract
The ability of coffee husks (CHs) and corn cobs (CCs) as biosorbents for methylene blue (MB) was investigated in batch mode. The energy dispersive X-ray spectroscopy was used for the determination of elemental composition of both biosorbents. Sorption experiments were carried out as a function of temperature, pH and MB initial concentration. Adsorption capacities of both materials significantly increased with the MB initial concentration. Among the various kinetic and adsorption isotherm models, the experimental adsorption data were best fitted in pseudo-second-order kinetic model and Langmuir isotherm model. The maximum adsorption capacities at room temperature were found to be 79.60 and 73.16 mg g^{-1} for CHs and CCs respectively. Moreover, the great affinity of MB towards CHs led to deep electrochemical experiments shown that CHs can be used as prominent modifier for a carbon paste electrode (CPE). The linear dynamic range of MB was found within the concentration range of 1–125 µmol/L with a detection limit (3σ) of 3 µM. The elaborated sensor was successfully applied for the determination of adsorption capacities of CHs placed into a column for MB biosorption in river water, suggesting that CH-CPE could be an efficient tool for MB detection in environmental samples.

Keywords Isotherm · Biosorbent · Voltammetry · Electroanalysis · Carbon paste electrode

1 Introduction

The daily and intensive use of dyes remains nowadays a threat for human beings and microorganisms, for both vegetal and animal origins. Dyes are widely used in textiles, paper, rubber, plastics, leather, cosmetics, pharmaceutical and food industries. Environmental pollution by that class of compounds is mainly due to the discharge of industrial wastewater into surrounding water and natural streams [1]. Dyes usually have a synthetic origin and complex aromatic molecular structures which make them more stable and more difficult to biodegrade [2]. The discharge of coloured wastewater from previously mentioned industries has caused many significant problems such as the increase of the toxicity and chemical oxygen demand (COD) of the effluent, and also the reduction of light penetration, which has a derogatory effect on photosynthetic phenomena [3].

Methylene blue (MB, Scheme 1) also called methylthioninium chloride, is a cationic dye of the xanthine family. MB has wider applications, which include colouring paper, temporary hair colorant and coating for paper stock. It is one of the most consumed dyes in textile industry, used for cotton and silk painting [4].

It is also widely exploited in various fields related to chemistry and biology [5] where it is associated with the

✉ Evangeline Njanja, njanja.tcheunkeu@univ-dschang.org | [1]Electrochemistry and Chemistry of Materials, Department of Chemistry, University of Dschang, P.O. Box 67, Dschang, Cameroon. [2]SFR ICAT, Laboratoire GEIHP EA 3142, Institut de Biologie en Santé, Université d'Angers, 4 Rue Larrey, 49933 Angers Cedex 9, France. [3]PBH-IRIS, CHU, Université d'Angers, 4 Rue Larrey, 49933 Angers Cedex 9, France. [4]Laboratoire d'Analyses Industrielles et Génie des Matériaux, Département de Génie des Procédés, Faculté des Sciences et de la Technologie, Université 8 Mai 1945 Guelma, BP 401, 24000 Guelma, Algeria.

SN Applied Sciences (2019) 1:513 | https://doi.org/10.1007/s42452-019-0520-6

Received: 3 January 2019 / Accepted: 24 April 2019 / Published online: 3 May 2019

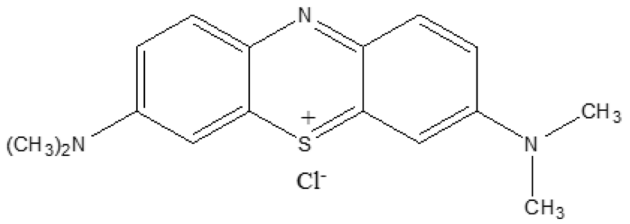

Scheme 1 Structure of methylene blue

determination of glucose, oxygen and ascorbic acid [6]. Though MB is not strongly hazardous, it can cause some harmful effects. Acute exposure to MB will cause increased heart rate, vomiting, shock, Heinz body formation, cyanosis, jaundice, quadriplegia, and tissue necrosis in humans [3]. When inhaled or ingested, it can cause nausea, diarrhoea, gastric, severe headache or mental disorder [7]. To deal with these problems, various conventional methods have been developed to eliminate colorants from industrial effluents. They include reduction followed by chemical precipitations [8], ion exchange [9], inverse osmosis [10], coagulation and flocculation [11], oxidation or ozonation [12], membrane separation [13] and adsorption on activated commercial charcoal [14, 15]. Most of these methods are however expensive, especially when applied to effluents with high flow rates or high concentration of dyes. The literature reports many studies on MB adsorption on activated carbons, the most common adsorbent used [16, 17]. However, the cost of this material is the main limitation for its intensive use [18]. As substitution materials, clays have been the subject of numerous research studies and the results obtained so far are often comparable to those obtained with activated carbon [19–21]. In recent years, a new class of biosorbents and specifically lignocellulosic materials have been investigated for the same purposes, their attractiveness resulting from their great availability, low cost, biodegradability and organophilic character. Yet, some preliminary studies have shown the ability of this class of materials to quantitatively accumulate organic compounds such as dyes [22] and pesticides [23]. The uptake of such organic compounds is commonly achieved via the hydroxyl and carbonyl groups found abundantly in polysaccharides (cellulose and hemicelluloses) and lignin [19]. In Cameroon characterized by intense agricultural activities, large amounts of CHs and CCs are produced annually but their applications as soil fertilizers, livestock feed or compost are still limited. By contrast, a common practice consists to burn or to dump these agricultural by-products into environment.

On the other hand, the monitoring of water contaminated by dyes is of great importance, both from analytical and environmental points of view. As for common electro active organic compounds, one could reasonably develop amperometric sensing devices useful in the quantification of such a dye. Yet, amperometric sensors are cost effective, require simple operations and are usually sensitive for the detection at very low concentration of analytes. In that field, carbon paste electrodes (CPEs) have been shown as attractive tool due to some of their typical properties such as low background currents, long-time stability, high polarization limits, easy fabrication and comfortable renewal of the paste [24]. In connection with electrochemistry, MB has been usually used as indicator [25] and as electron mediator or hybridization agent system in biosensing analysis [26–29]. Only few works have been also reported on the electroanalysis of MB, that include the investigation by cyclic voltammetry of the electrochemical behavior of MB at a carbon fibre micro cylinder electrode [30] and the determination of MB at a thiol functionalized-clay CPE [31]. Obviously, the development of simple and low-cost procedure for the quantification of MB is still necessary. Therefore, the purpose of the present study was first to evaluate the biosorption ability of two lignocellulosic materials, CHs and CCs for the uptake of MB in aqueous solution. Key parameters likely to influence the sorption of MB by the investigated materials were analysed and optimised. Secondly, the possibility of using a carbon paste electrode chemically modified by CHs as amperometric sensor for the detection of MB was also investigated. The detection limit of the elaborated sensor for MB detection was clearly established. Finally, the tested electrode was successfully applied for the evaluation of MB biosorption in river water on column, using CHs as adsorbent.

2 Materials and methods

2.1 Reagents, chemicals and apparatus

A stock solution of MB was prepared by dissolving in distilled water MB (98%, BDH-Prolabo). Homogenization of the solutions was carried out by using an Edmund Bühler GmbH SM-30 shaking table. The residual concentrations of MB after biosorption were measured using a JENWAY spectrophotometer. A 0.1 M phosphate buffer solution (PBS) at pH 7.4 prepared from KH_2PO_4 and K_2HPO_4 (both from Sigma-Aldrich) was used as supporting electrolyte in the electrochemistry section. NaCl, HCl (37%), NaOH and MeOH were of analytical reagent grade and used as received. When necessary, 0.1 M NaOH and 0.1 M HCl were used to adjust the pH of the solutions. Energy dispersive X-ray spectroscopy (EDX) experiments was achieved by Field Emission Gun Scanning Electron Microscopy (FEG-SEM) on a JSM-6301F apparatus from JEOL (SCIAM, University of Angers, France). Images obtained were

from secondary electrons of 3 keV, with magnifications between ×25 and ×20,000 and the beam energy was 20 keV.

2.2 Biosorbents and pretreatment

CHs and CCs selected for this study as biosorbents were obtained from local agricultural units, in Dschang (Menoua Division, West-Cameroon). Each of these materials was sun dried until a fixed mass was obtained. They were ground and crushed, and a series of sieves allowed to obtain their fine fractions (0–100 µm). To remove the extractives which may reduce their adsorption capacities, 2 g of each biosorbent were washed several times with distilled water and then soaked for 2 h in 30 mL of MeOH. After washing again thoroughly with distilled water, biosorbents were once more sun dried for 2 days and then in an oven at 105 °C for 2 h. The biosorbents obtained at the end of this process were used without further treatment for the biosorption of MB.

2.3 Determination of the macromolecular composition of biosorbents

An estimation of the three parietal constituents (cellulose, hemicellulose and lignin) contained in the CCs and CHs was made using ADF-NDF method of Van Soest and Wine [32, 33]. Solubility in the ADF, NDF and ADF-$KMnO_4$ solutions was also extrapolated. Solubilisation and filtration were done in a Fibretec M2 system, equipped with a heating and reflux device (from FOSS, France). All determinations were carried out in duplicate.

2.4 Batch biosorption experiments

Biosorption experiments were carried out in batch mode. Thus, 10 mg of each biosorbent treated as indicated above were weighed and introduced into 25 mL flask containing 15 mL of a solution of a given concentration of MB. A series of flasks were prepared by varying the parameters to be investigated. They were placed in a mechanical platform shaker (Edmund Bühler, GmbH) and stirred for a determined period at a speed of 200 rpm. A flask without biosorbent was stirred under the same conditions as a control. After stirring, the flaks were allowed to rest for a few minutes, a part of the solution from the upper liquid layer was removed using a micropipette and the MB residual concentration was determined by spectrophotometric analysis. The effect of biosorbent mass on the adsorption of MB was studied for the concentration range 0.6–4.6 g L^{-1}, corresponding to 10–70 mg in 15 mL of 5×10^{-5} mol L^{-1} MB.

The amount of MB adsorbed at equilibrium per unit mass of adsorbent (q_e (mol g^{-1})) and the percentage adsorbed ($\%_{ads}$) were determined using Eqs. (1) and (2):

$$q_e = \frac{(C_0 - C_e)}{m} Vs \quad (1)$$

$$\%_{ads} = \frac{(C_0 - C_e)}{C_0} 100 \quad (2)$$

where C_0 (µmol L^{-1}) is the initial concentration of MB, C_e (µmol L^{-1}) is the residual concentration of MB in solution at equilibrium, V_s (L) the volume of solution and m (g) the mass of the biosorbent.

2.5 Electrochemical procedures and equipment

Electrochemical measurements were performed using a PG580 potentiostat (Uniscan Instruments, UK) connected to a personal computer. A conventional three-electrode cell configuration was employed, consisting of bare or modified carbon paste electrode (CPE) serving as working electrode, a saturated calomel reference electrode (SCE) and a platinum wire counter electrode. The CPE was prepared according to a well-known procedure [34]: briefly, 70 mg of graphite powder (analytical grade, ultra F, < 325 mesh, from Alfa) and 30 mg of silicone were thoroughly hand-mixed in a mortar. A portion of the composite mixture was packed into the cylindrical hole of a Teflon tube equipped with a copper wire serving as electrical contact with the rest of the circuit. The active surface of the electrode was polished on a weighing paper for renewing the surface after each analysis. CHs modified CPEs (CH-CPE) were prepared as described for the bare CPE, by using 65 mg of graphite powder, 30 mg of silicone oil and 5 mg of CH powder (10 µm average size).

Cyclic voltammetry was used to investigate the electrochemical behaviour of MB on the bare CPE and CH-CPE. Square wave voltammetry (SWV) was used as analytical technique to evaluate the ability of CH-CPE for the detection in aqueous solution of MB. The optimized SWV parameters were frequency 400 Hz, pulse height 90 mV and scan increment 15 mV.

3 Results and discussion

3.1 EDX and SEM characterization of different electrodes

The EDX spectra of pristine CHs and CCs are shown in Fig. 1. As seen in Fig. 1a, b, both spectra are very similar.

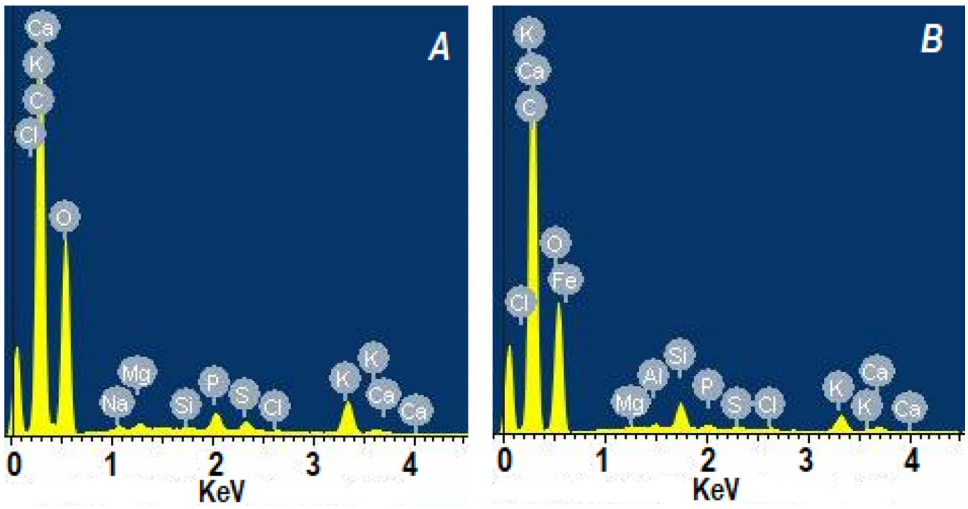

Fig. 1 EDX spectra of **a** CHs and **b** CCs

They present almost the same chemical elements, proving that both CHs and CCs have similar chemical compositions.

As most of lignocellulosic materials, CHs and CCs are constituted mainly of cellulose, lignin and hemicellulose, which could be represented on the EDX spectra (Fig. 1) by the presence of chemical elements such as carbon and oxygen. In addition of the three components mentioned above, the literature report of extractives (tannins, pectins, polymers of low degree of polymerization) and minerals [35–38] in lignocellulosic materials composition. As seen in Fig. 1, minerals such as Ca^{2+}, K^{+}, Cl^{-}, Na^{+}, Mg^{2+}, Al^{3+} are clearly identified and known to be the potential minerals commonly found in lignocellulosic materials. This section opens a way for further characterisations of CHs and CCs notably an estimation of the amounts of cellulose, hemicellulose and lignin.

3.2 Determination of the macromolecular composition of biosorbents

The percentages of cellulose, lignin and hemicelluloses in pristine CHs and CCs were estimated using ADF-NDF method. For CHs, cellulose, lignin and hemicellulose accounted for 55.1%, 9.2% and 0.1% respectively, meanwhile CCs showed percentages of 53.4, 43.7 and 2.9 respectively for cellulose, hemicellulose and lignin in the total dry weight. Looking the obtained values, it can be noted that in CHs hemicellulose was almost absent. Despite the absence of hemicellulose from the obtained results, the percentages of cellulose and lignin were in close agreement with those reported for the analysis of CHs originating from Portugal [39]. Thus, it is important to mention that the composition of lignocellulosic materials greatly depends on several parameters including the geographic location, the age of vegetable and the soil composition [40].

3.3 Effect of contact time

The contact time is the time necessary for equilibrium to be attained between the pollutant and the biosorbent, indicating the end of the adsorption process. Since adsorption is a process that involves the transfer of pollutant from the liquid phase to the solid phase, the contact time between both phases has a great effect on the amount of material transferred. The variations occurring in the liquid phase were studied using the batch method.

For each biosorbent, Fig. 2 presents the adsorption kinetics expressed as the variation over contact time of the quantity of MB adsorbed per gram of material. It can be noticed that the adsorption is fast, with chemical equilibrium attained within the first 20 min. Figure 2 clearly shows an increase in the uptake of MB by both materials

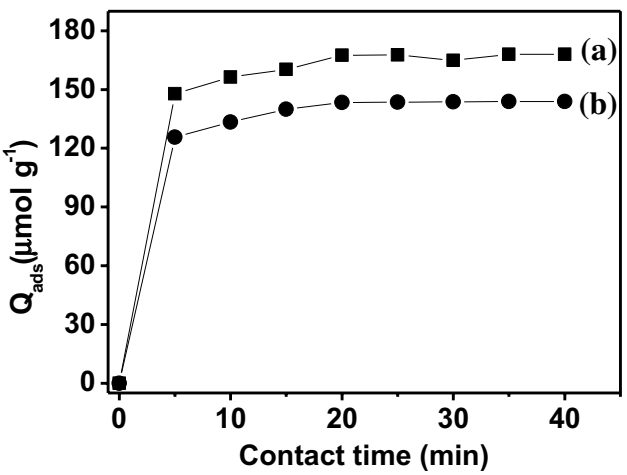

Fig. 2 Adsorption kinetics of MB on (a): CHs and (b): CCs. (Experimental conditions: Adsorbent dosage, 0.66 g L^{-1}; MB concentration, 5×10^{-5} M; biosorbent particle size, 0–100 µm; pH 6 at a temperature of 25 °C)

as the contact time increases. It can be noticed that these curves are saturation curves, which can be divided into two parts: the first part of the curve (contact time less than 20 min) represents a rapid process while the second part is fairly rapid, traducing a saturation of adsorbing sites [41].

3.4 Effect of the initial concentration of pollutant

The initial concentration of pollutant can influence the retention capacity of the solid supports used as adsorbents. Figure 3 shows the amount of MB adsorbed by the investigated materials under different initial MB concentrations. One can observe that the retention of MB by the biosorbents is influenced by the initial concentration of MB. In general, the adsorption capacity increases with an increase in the initial concentration of MB. This may be explained by the fact that an increase in the concentration of pollutant increases competition for the occupation of adsorption sites of the biosorbent. This occupation of adsorption sites of the biosorbent continues until equilibrium is attained, leading to saturation. At this point, the energetically active sites involved in the adsorption process are saturated and the curves attain a plateau. It can also be noted that the CHs have a higher adsorption capacity than that of CCs. The adsorption sites of CHs are probably greater in number and more active than those of CCs. The increase in amount of adsorbed pollutant becomes less important when the initial concentration of MB is raised, due to the reduction of bindings sites.

The plateau which appeared for initial concentrations above (144 and 168 µmol g^{-1}, respectively for CCs and CHs) indicated that the biosorption process reached equilibrium and that all adsorption sites are occupied. These observations are very common during adsorption studies [19, 31].

3.5 Effect of adsorbent dosage

In order to investigate the effect of adsorbent dosage, MB uptake was evaluated using different ratios between biosorbent mass (g) and volume (L) of MB solution (adsorbent dosage). The behaviour of adsorption capacity in function of adsorbent dosage is plotted in Fig. 4.

Along with the adsorbent dosage increase from 0.06 to 2 g L^{-1}, the adsorption capacity decreased from 405 to 105 and from 340 to 85 µmol g^{-1} for CHs and CCs respectively. For constant initial dye concentration, with increasing the adsorbent dosage the interfacial tension between both phases increases and, as a consequence, the driving force for the mass transfer decreases, reducing in this way the adsorption capacity. It is worth noting that the high specific surface area and porosity of both biosorbents conferred a great removal efficiency of dye also at relatively low adsorbent dosages as stated by previous works [42–45].

3.6 Effect of biosorbent particle size

The influence of the particle size of each biosorbent on its capacity to retain MB was also studied. To better illustrate the effect of particle size, the quantities adsorbed are represented as a function of the nature of biosorbent. The histogram in Fig. 5 shows the adsorption capacity of each of the biosorbents for diameters in the ranges 0–100, 100–200 and 200–300 µm, respectively. It was observed that the retention of MB increases when the particle size

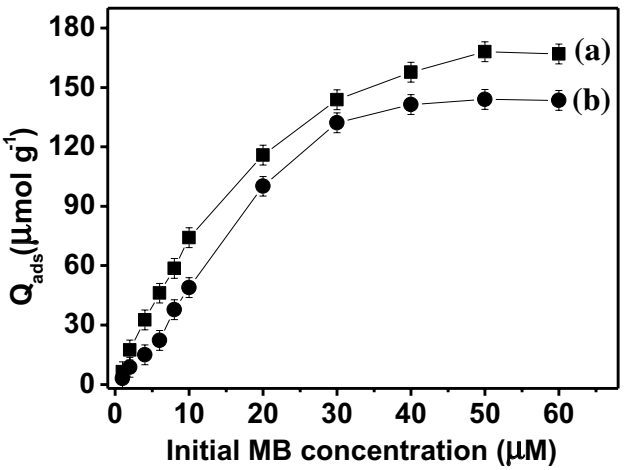

Fig. 3 Effect of MB initial concentration (C_0) on the biosorption capacity of (a): CHs and (b): CCs. (Experimental conditions: Adsorbent dosage, 0.66 g L^{-1}; shaking time, 40 min; biosorbent particle size, 0–100 µm; pH 6 at a temperature of 25 °C)

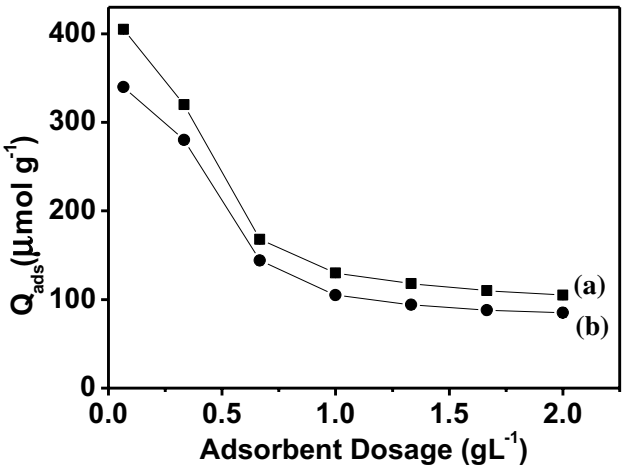

Fig. 4 Effect Adsorbent dosage on the biosorption capacity of (a): CHs and (b): CCs. (Experimental conditions: MB concentration, 5×10^{-5} M; shaking time, 40 min; biosorbent particle size, 0–100 µm; pH 6 at a temperature of 25 °C)

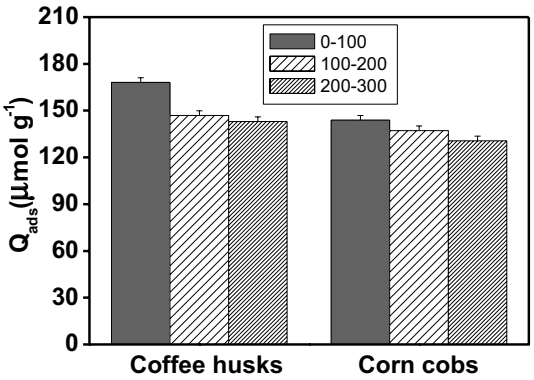

Fig. 5 Influence of particle size of CHs and CCs on the adsorption of MB. (Experimental conditions: Adsorbent dosage, 0.66 g L^{-1}; MB concentration, 5×10^{-5}M; shaking time, 40 min; pH 6 at a temperature of 25 °C)

decreases. This is due to the fact that fine particle size provides large surface area of contact, facilitating the fixation of MB on the adsorption sites of the biosorbents. On the other hand, access to these adsorption sites becomes difficult when particle size increases, diffusion being reduced by the ligneous matrix.

3.7 Effect of temperature

In order to study the effect of temperature on the adsorption process of MB onto CHs and CCs, experiments were carried out at temperatures of 20, 25, 30, 40 and 50 °C. Figure 6 shows the influence of temperature on the adsorption capacity of each biosorbent. In particular, the adsorption capacity slightly decreased when the temperature increases. This suggests that the interactions between the cationic dye and active functional groups of both biosorbents were lower at higher temperatures.

3.8 Effect of the pH

Since the adsorbent charge is closely dependent on the acidity of the solution [46, 47], the pH is a key factor as far as adsorption of cationic compounds is concerned. We have thus studied the efficiency of the adsorption when the pH is varied. Figure 7 shows the behavior of the adsorption capacity of both biosorbents as function of pH.

As can be seen, the adsorption capacity increased with increase of the pH up to 10. This can be explained by the fact that for acidic pH values, the biosorbent get the positive charge due to the protonation of carboxylate groups present in its surface [48]. Electrostatic repulsions then prevent the protonated material and MB (positively charged) to interact efficiently. However, for high values of pH, the biosorbent losses the proton which favours its attraction with pollutant [31].

3.9 Adsorption isotherms study

The adsorption isotherms study, through the fitting of the isotherm experimental data with different isotherm models is important for the description of the adsorption process and it is critical in optimizing the use of an adsorbent. Several mathematical models can be used to fit the experimental adsorption values: in this work the Langmuir, Freundlich and Temkin models were employed for the interpretation of experimental data (Fig. 8).

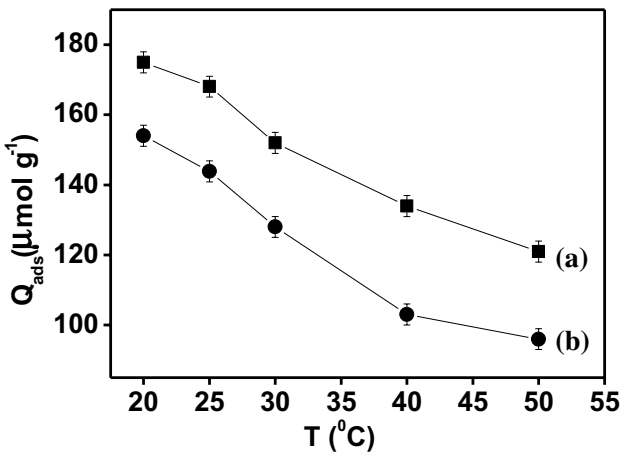

Fig. 6 Effect of temperature on the MB biosorption. (a): CHs and (b): CCs. (Experimental conditions: Adsorbent dosage, 0.66 g L^{-1}; MB concentration, 5×10^{-5} M; biosorbent particle size, 0–100 µm; shaking time, 40 min; pH 6)

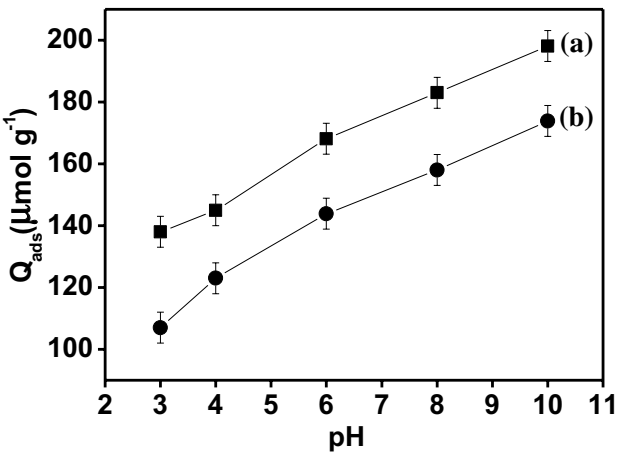

Fig. 7 Effect of pH on the MB biosorption. (a): CHs and (b): CCs. (Experimental conditions: Adsorbent dosage, 0.66 g L^{-1}; MB concentration, 5×10^{-5} M; biosorbent particle size, 0–100 µm; shaking time, 40 min; temperature, 25 °C)

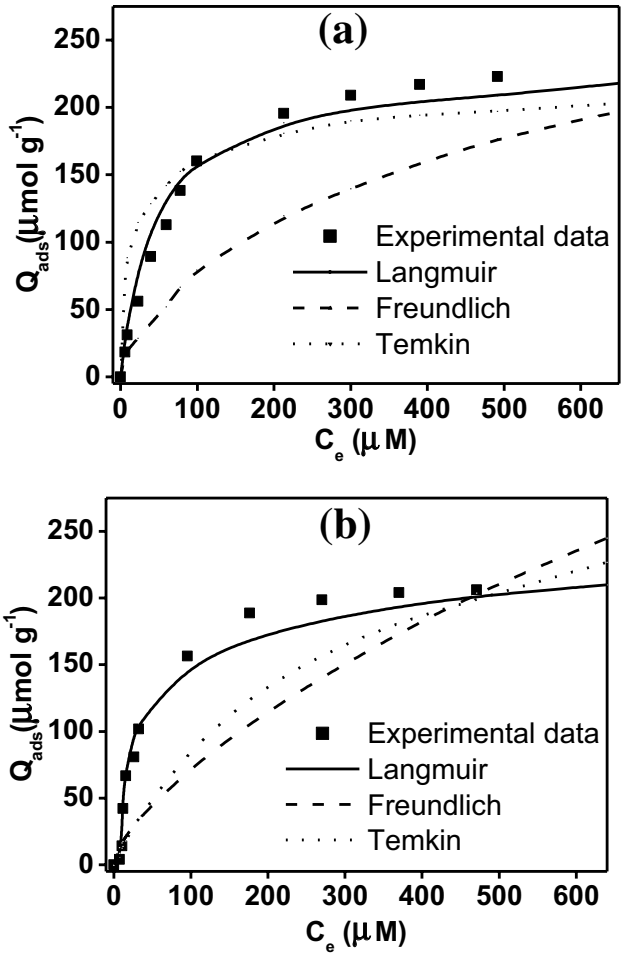

Fig. 8 Comparison of Langmuir, Freundlich and Temkin MB adsorption isotherms fitted to experimental data. **a** CCs and **b** CHs

The Langmuir adsorption isotherm, which assumes that the adsorption occurs at specific homogeneous sites within the adsorbent and which has been successfully applied to many monolayer adsorption process [49], can be written using the following linearized Eq. (3):

$$\frac{C_e}{Q_e} = \frac{1}{Q_{\max}} C_e + \frac{1}{K_L Q_{\max}} \tag{3}$$

where Q_e (mol g^{-1}) is the adsorption capacity at equilibrium, Q_{max} (mol g^{-1}) is the maximum adsorption capacity, C_e (mol L^{-1}) is the equilibrium concentration of MB in solution and K_L (L mol^{-1}) is the effective dissociation constant.

The Freundlich isotherm, which describes the adsorption process on an energetically heterogeneous surfaces, can be written using the following linearized Eq. (4):

$$\ln Q_e = \ln K_F + \frac{1}{n} \ln C_e \tag{4}$$

where K_F (mol^{1-n} L^n g^{-1}) is a constant indicative of the adsorption capacity of the adsorbent and n is an empirical constant related to the magnitude of the adsorption driving force.

Finally, the Temkin model is based on the assumption that some indirect sorbate/adsorbate interactions are responsible of the linear decrease of the adsorption heat of all the molecules in the layer with coverage. The Temkin isotherm is generally presented by the following Eq. (5):

$$Q_e = Q_{\max} \frac{RT}{\Delta Q} \ln(K_T C_e) \tag{5}$$

where Q_{max} (mol g^{-1}) and K_T (L mol^{-1}) are Temkin constants, R is the ideal gas constant (8.314 J mol^{-1} K^{-1}), and T (K) is absolute temperature.

For CHs and CCs materials, the Langmuir, Freundlich and Temkin isotherm models are illustrated in Fig. 8, while the corresponding constants are gathered in Table 1.

In Table 1, the parameter values of the applied isotherms and the related correlation coefficient R^2 are reported. As can be seen, the Langmuir model showed the higher R^2 value (0.998 for CCs, and 0.0995 for CHs), suggesting that this model yielded the best fit compared to other models. By using the Langmuir isotherm, it is possible to predict whether an adsorption system is favorable or unfavorable through a dimensionless constant referred to as separation factor R_L defined by the following Eq. (6).

$$R_L = \frac{1}{1 + K_L C_0} \tag{6}$$

where K_L (L µmol^{-1}) is the Langmuir constant and C_0 (mol L^{-1}) is the initial concentration of MB in solution. The value of R_L indicates if the adsorption process is irreversible ($R_L = 0$), favorable ($0 < R_L < 1$), linear ($R_L = 1$) or unfavorable ($R_L > 1$). R_L values related to MB adsorption on both biosorbents were less than 1 and greater than 0 for all initial MB concentration considered (Fig. 9), indicating a favorable adsorption.

The constant value 1/n, determined by the Freundlich model (0.667 for CHs and 0.396 for CCs) between 0 and 1 is an indication of the affinity of biosorbents for MB. Looking at these values of 1/n, it is clear that CHs have a better affinity with MB compared to CCs, indicating that CHs adsorption sites are more active than those of CCs.

Temkin's model was used to determine the different heats of adsorption involved during various adsorbate-adsorbent interactions. There is a little variation of heat with the CCs (11.979 kJ µmol^{-1}) compared to CHs (12.818 kJ µmol^{-1}). This may reflect the fact that interactions between MB and CHs are more energetic than those between MB and CCs.

Table 1 Langmuir, Freundlich and Temkin constants

Biosorbents	Isotherms types	Constants	
Corn cobs	Langmuir	Q_{max} (μmol g^{-1})	227.273 ± 0.004
		K_L (L μmol^{-1})	0.023 ± 0.006
		R^2	0.998 ± 0.009
	Freundlich	1/n	0.396 ± 0.04
		K_F (μmol^{1-n} L^n g^{-1})	8.331 ± 0.09
		R^2	0.921 ± 0.06
	Temkin	ΔQ (kJ μmol^{-1})	11.979 ± 0.0002
		K_T (L μmol^{-1})	− 3.944 ± 0.0003
		R^2	0.981 ± 0.0006
Coffee husks	Langmuir	Q_{max} (μmol g^{-1})	304.878 ± 0.007
		K_L (L μmol^{-1})	0.004 ± 0.001
		R^2	0.995 ± 0.008
	Freundlich	1/n	0.666 ± 0.07
		K_F (μmol^{1-n} L^n g^{-1})	3.384 ± 0.02
		R^2	0.994 ± 0.08
	Temkin	ΔQ (kJ μmol^{-1})	12.818 ± 0.0003
		K_T (L μmol^{-1})	− 3.029 ± 0.0003
		R^2	0.967 ± 0.0005

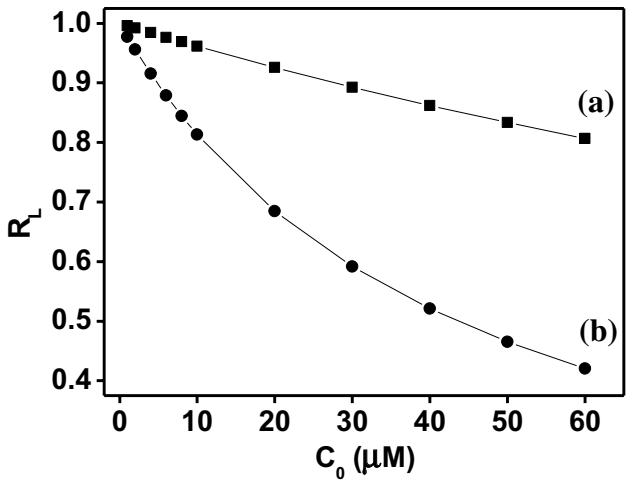

Fig. 9 Separation factor for the adsorption of MB on (a): CHs and (b): CCs

Although the Langmuir model is rather common for the biosorption of organic polluants [19–23, 50–54], it is difficult to compare the Q_{max} values of the various adsorbents because the experimental conditions have to be identical which is not the case herein, the studies have been carried out independently. In Table 2, are gathered the values of maximum adsorption capacities obtained for the adsorption of MB onto various adsorbents. Comparing to the other adsorbents, the obtained adsorption capacities of CCs and CHs are relatively high while, CHs are significantly more efficient.

Table 2 Maximum adsorption capacities obtained for the adsorption of methylene blue onto various adsorbents

Adsorbents	Q_{max} (mg g^{-1})	References
Mansonia wood sawdust	16.21	[19]
Kenaf Care Fibers	44.84	[20]
Jack Fruit Peel	10.58	[21]
Activated Carbon	9.81	[51]
Purified Clay	68.49	[52]
Charcoal	62.70	[53]
Corn cobs	19.72	[54]
Raw Corn Cobs	18.28	[55]
Coffee Husks	90.1	[56]
Corn Cobs	72.61	This Work
Coffee Husks	97.41	This Work

3.10 Adsorption kinetics

The adsorption kinetics, that shows the evolution of the adsorption capacity during time, also helps to understand the types of adsorption mechanism of a system. The experimental values of adsorption capacities collected during time using the solution at initial MB concentration of 5×10^{-5} M were fitted using the pseudo-first order and pseudo-second order models.

The linearized forms of pseudo-first order and pseudo-second order kinetic models are shown by Eqs. (7) and (8) respectively, where k_1 (min^{-1}) and k_2 (L μmol^{-1} min^{-1}) are rate constants of adsorption, q_t (L μmol^{-1}) is

the adsorption capacity at time t, q_e (L μmol^{-1}) is the equilibrium adsorption capacity.

$$\log(q_e - q_t) = \log q_e - \frac{k_1}{2.303}t \quad (7)$$

$$\frac{t}{q_1} = \frac{1}{k_2 q_e^2} + \frac{1}{q_e}t \quad (8)$$

All the constants related to these models are summarized in Table 3

The adsorption process was best described by the pseudo-second order kinetic model for both biosorbents ($R^2 > 0.999$). Also, the calculated values of adsorption capacities (q_e) were very close to the experimental ones (q_{exp}).

The applicability of the pseudo-second order model suggests that chemical reactions were responsible for the adsorption of MB on both biosorbents.

3.11 Thermodynamic parameters

The free energy change (ΔG°), enthalpy change (ΔH°), and entropy change (ΔS°) were determined in order to evaluate the effect of temperature on MB adsorption by CCs and CHs. The Gibbs free energy was evaluated as:

$$\Delta G^o = -RT \ln k \quad (9)$$

where ΔG° is the standard Gibbs free energy change (kJ mol^{-1}), R and T have the same signification as previously, and k is the apparent equilibrium constant, defined as:

$$k = \frac{q_e}{C_e} \quad (10)$$

where C_e and q_e, correspond to the equilibrium concentration of MB on the solution and on the adsorbent, respectively. The Van's Hoff equation is expressed as follows:

$$\ln k = \left(\frac{\Delta S^\circ}{R}\right) - \left(\frac{\Delta H^\circ}{R}\right)\frac{1}{T} \quad (11)$$

where ΔS° and ΔH° are entropy change and enthalpy change, respectively. The plot of lnk versus 1/T gives a linear relationship, which allows the computation of ΔH° and ΔS° values from the slope and the intercept, respectively. Results for thermodynamic parameters evaluation are displayed in Table 4.

It was observed that the values of ΔG° for the adsorption of MB onto CCs and CHs decreased with an increase in temperature suggesting a rapid and more spontaneous adsorption at the lower temperature. The negative

Table 4 Thermodynamic parameters for biosorption of MB onto CCs and CHs

	Temperature (°C)		
	20	25	50
Corn cobs			
k	2.924 ± 0.02	3.127 ± 0.02	6.855 ± 0.02
ΔG^0 (kJ mol^{-1})	− 2.658 ± 0.008	− 3.53 9 ± 0.007	− 4.569 ± 0.005
ΔH^0 (kJ mol^{-1})		− 0.245	
ΔS^0 (kJ mol^{-1} K^{-1})		0.020	
Coffee husks			
k	2.625 ± 0.03	2.709 ± 0.03	3.946 ± 0.03
ΔG^0 (kJ mol^{-1})	− 2.391 ± 0.009	− 2.797 ± 0.006	− 3.400 ± 0.006
ΔH^0 (kJ mol^{-1})		− 0.153	
ΔS^0 (kJ mol^{-1} K^{-1})		0.013	

Table 3 Adsorption kinetic parameters for the MB adsorption on CHs and CCs

Biosorbents	Kinetic models	Constants	
Corn cobs	Pseudo-first order	k_1 (min^{-1})	0.563 ± 0.03
		q_e (μmol g^{-1})	141.881 ± 0.06
		R^2	0.746 ± 0.03
	Pseudo-second order	k_2 (L μmol^{-1} min^{-1})	0.013 ± 0.006
		q_e (μmol g^{-1})	145.772 ± 0.003
		R^2	0.999 ± 0.008
		$t_{1/2}$ (min)	0.510 ± 0.002
Coffee husks	Pseudo-first order	k_1 (min^{-1})	0.213 ± 0.02
		q_e (μmol g^{-1})	165.043 ± 0.08
		R^2	0.954 ± 0.05
	Pseudo-second order	k_2 (L μmol^{-1} min^{-1})	0.009 ± 0.001
		q_e (μmol g^{-1})	169.779 ± 0.005
		R^2	0.999 ± 0.008
		$t_{1/2}$ (min)	0.6451 ± 0.002

ΔH° value obtained confirms the exothermic nature of the adsorption process. The obtained positive value of ΔS° reveals increased randomness at the solid/solution interfaces and good affinity of the adsorbents for MB [56].

3.12 Electrochemical behavior of MB on CH modified CPE

Considering the good results obtained with coffee husks adsorbent over other materials (Table 2) and those from the previous section, we can state that CHs display a great affinity with MB. This has led us to explore the possibility to exploit the binding properties of CHs towards MB for its detection using voltammetric techniques. To this purpose, CHs were successfully inserted into the carbon paste. Cyclic voltammetry (CV) was first used to characterize the electrochemical behavior of MB and to compare its voltammetric response on the bare CPE and CH-CPE, in 0.1 M PBS (pH 7.4) at a scan rate of 100 mV s^{-1} as seen in Fig. 10.

A pair of reversible peaks was obtained for MB corresponding to its oxidation (around − 0.13 V versus SCE) followed by its reduction (at − 0.22 V) upon potential reverse scan according to the following Scheme 2.

In fact, the oxidation response of MB on CH-CPE was observed to be more pronounced than that recorded on the bare CPE (Fig. 10). The difference observed between peak currents is due to the presence of CHs which increase the real surface area and improve the hydrophilic character of the modified electrode as previously demonstrated [57, 58]. In addition, CHs are mainly constituted of cellulose that having hydrophilic character could easily interact with MB which is also a hydrophilic molecule [57].

The obtained results have led us to further investigate the possibility of using the CH-CPE to propose a more sensitive procedure for the determination of MB in aqueous solutions. Figure 11 compares typical SWV curves of 25×10^{-6} M MB on the bare CPE before and upon modification using CHs.

Compared to the bare CPE, the oxidation peak current of MB was increased by a factor of 2.5 on the CH-CPE (Fig. 11). As already revealed by cyclic voltammetry studies, the observed behavior of MB is attributed to the enhancing action of CHs at the surface of the electrode, which favour the accumulation of MB, thereby leading to a great amperometric response. This point out the great affinity of CHs towards the accumulation of MB. Thus, the obtained results suggest that CH-CPE can be used as an electrochemical sensor for MB.

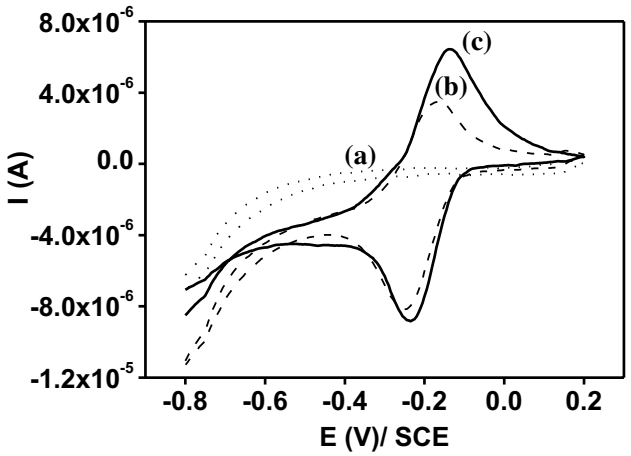

Fig. 10 Cyclic voltammograms (a) at CPE in 0.1 M PBS (pH 7.4), and of 25×10^{-6} mol L^{-1} MB in 0.1 M PBS (pH 7.4) (b) at the bare CPE and (c) at CH-CPE. Potential scan rate: 100 mV s^{-1}

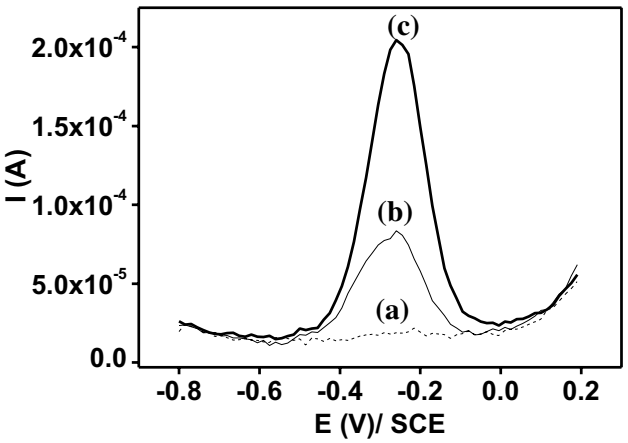

Fig. 11 Square wave voltammograms (a) at CPE in 0.1 M PBS (pH 7.4), and of 25×10^{-6} mol L^{-1} MB in 0.1 M PBS (pH 7.4) at the bare CPE (b) and at the CPE modified by coffee husks (c). Potential scan rate: 100 mV s^{-1}

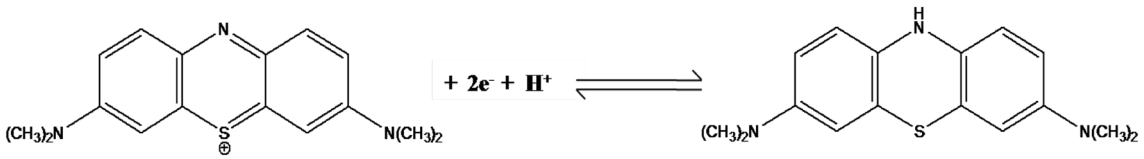

Scheme 2 Electrochemical oxidation of MB

3.13 Calibration curve and limit of detection

To a great extent, the SW peak current at that lignocellulosic modified carbon paste electrode was recorded as a function of MB concentration. Figure 12 depicts the curves obtained under SWV optimized conditions in PBS in the concentration range of 1–125 µM, while the inset in the same figure presents the evolution of peak current as a function of MB concentration.

Over the investigated MB concentration, a linear dependence was observed between both parameters, with the following equation: Ip (A) = 6.9×10^{-6}[MB] (µM) + 1.1×10^{-5} ($R^2 = 0.999$), and a sensitivity of 6.93×10^{-6} A/µM. The limit of detection was calculated to be 3 µM using 3S/b, where S is the standard deviation of the blank and b is the slope of the calibration curve.

3.14 Interference study

The interference of some species on the electrochemical determination of MB with CH-CPE was investigated under optimum condition. The selected interfering ions such as Na^+, Ca^{2+}, Ba^{2+}, K^+, Al^{3+}, Cl^-, NO_3^-, Mg^{2+} were studied, since they are usually present in natural rivers water. Indeed, a known amount of each studied species was added to a 25 µM MB solution and the obtained solutions were analysed by SWV. The limit of tolerance was defined as the foreign ion concentration causing an error smaller than 3.0% for the determination of MB and the investigations showed that there is no interference from these species on the determination of MB.

3.15 Application of the proposed method using river water sample

To study the applicability of the proposed method, the CH-CPE was finally applied successfully to evaluate the adsorption capacity of MB on CHs placed into a column. In fact, a sample of river water was doped with a known amounts of MB and transferred into an adsorption column using CHs as adsorbent. The passage of MB solution into the column was effective after 45 min. Residual MB solutions were then determined by SWV on CH-CPE. The obtained results are summarised in Tables 5.

In Table 5, the adsorption capacities of CHs obtained on column and determined through voltammetric method using CH-CPE were comparable to those achieved from batch process using the spectrophotometric method. In fact, the adsorption capacities obtained on column were relatively greater than those achieved by batch process. This may be attributed to the fact that, many interactions from shaking effect intervene during the batch process between the pollutant and adsorbent, by reducing the adsorption capacities of biosorbents. On the contrary, in column process, no interactions are occurring between both adsorbent and pollutant indicating that column process coupled to voltammetric methods could be the better ways for MB adsorption on CHs. The obtained results suggest also

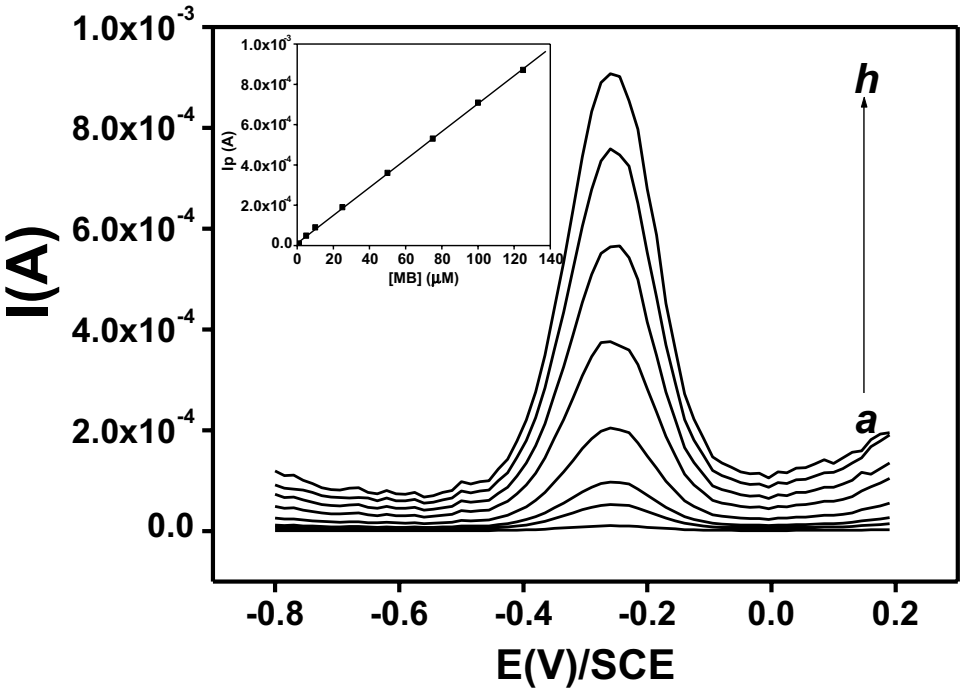

Fig. 12 SWV of MB at different concentrations in 0.1 M PBS (pH 7.4) on the CH-CPE. MB concentration (a–h): 1, 5, 10, 25, 50, 75, 100 and 125 µM. Inset shows the evolution of peak current as a function of MB concentration

Table 5 Determination of MB in river water and comparison of CHs adsorption capacities obtained on both column and batch processes

MB initial concentrations (μM)	Residual MB concentrations (μM)	Adsorption capacities of CHs on column (μmol/g)	Adsorption capacities of CHs on batch mode (μmol/g)
10	6.37	5.45	3.88
20	9.44	15.84	14.04
40	10.8	43.80	42.10
60	14.39	68.42	66.61
80	24.95	82.58	80.82

that the present sensor using CHs as modifier, may be an efficient tool for MB determination in real samples.

4 Conclusion

In this study, biosorption experiments for the uptake of methylene blue from aqueous solutions have been comparatively carried out using coffee husks and corn cobs as low-cost and natural available biosorbents. It was found that the investigated biosorbents quantitatively adsorb the dye with a very fast kinetics (equilibrium was reached for both materials within the first 20 min). The sorption of MB was shown to be dependent on the biosorbent particle size, adsorbent dosage, temperature, pH and on methylene blue initial concentration. Coffee husks demonstrated great affinity towards the dye, and the biosorption on that material proceed by the formation of a monolayer as shown by the good correlation with the Langmuir adsorption model. This allowed the use of coffee husks as a carbon paste electrode modifier for the electrochemical detection of methylene blue by cyclic voltammetry and square wave voltammetry. The obtained results showed that coffee husks modifier electrode exhibited a good stability and excellent sensitivity towards the detection of MB. Finally, the elaborated sensor was successfully applied for the determination of adsorption capacities of CHs on column process, suggesting that coffee husks could be an attractive and promising material for the development of both sensors and processes for environment purposes.

Acknowledgements The authors thank the support of The World Academy of Sciences for a support through the TWAS Research Grants Programme (Project n° 16-515 RG/CHE/AF/AC_G_FR3240293302). S. F. Mbokou was supported by ARIANES program (University of Angers, France).

Compliance with ethical standards

Conflicts of interest The authors declare that they have no conflicts of interest.

References

1. Marrakchi F, Ahmed JM, Khanday WA, Asif M, Hameed BH (2017) Mesoporous-activated carbon prepared from chitosan flakes via single-step sodium hydroxide activation for the adsorption of methylene blue. Int J Biol Macromol 98:233–239. https://doi.org/10.1016/j.ijbiomac.2017.01.119
2. Teli MD, Nadathur GT (2018) Adsorptive removal of Acid Yellow 17 (an anionic dye) from water by novel ionene chloride modified electrospun silica nanofibres. J Environ Chem Eng 8:8–9. https://doi.org/10.1016/j.jece.2018.10.005
3. Pathania D, Sharma S, Singh P (2017) Removal of methylene blue by adsorption onto activated carbon developed from *Ficus carica* bast. Arab J Chem 10:1445–1451. https://doi.org/10.1016/j.arabjc.2013.04.021
4. Lebron YAR, Moreira VR, Santos LVS, Jacob RS (2018) Remediation of methylene blue from aqueous solution by *Chlorella pyrenoidosa* and *Spirulina maxima* biosorption: equilibrium, kinetics, thermodynamics and optimization studies. J Environ Chem Eng. https://doi.org/10.1016/j.jece.2018.10.025
5. Pezoti O Jr, Cazetta AL, Souza FAPI, Bedin CK, Martins AC, Silva TL, Almeida VC (2014) Adsorption studies of methylene blue onto $ZnCl_2$-activated carbon produced from Buriti shells (*Mauritia flexuosa* L.). J Ind Eng Chem 20:4401–4407. https://doi.org/10.1016/j.jiec.2014.02.007
6. Thakur S, Pandey S, Arotiba AO (2016) Development of a sodium alginate-based organic/inorganic superabsorbent composite hydrogel for adsorption of methylene blue. Carbohydr Polym 153:34–46. https://doi.org/10.1016/j.carbpol.2016.06.104
7. Miraboutalebi MS, Nikouzad KS, Peydayesh M, Allahgholi N, Vafajoo L, McKay G (2017) Methylene blue adsorption via maize silk powder: kinetic, equilibrium, thermodynamic studies and residual error analysis. Process Saf Environ Protect 106:191–202. https://doi.org/10.1016/j.psep.2017.01.010
8. Giannopoulou I, Panias D (2008) Differential precipitation of copper and nickel from acidic polymetallic aqueous solutions. Hydrometallurgy 90:137–146. https://doi.org/10.1016/j.hydromet.2009.06.009
9. Alyüz B, Veli S (2009) Kinetics and equilibrium studies for the removal of nickel and zinc from aqueous solutions by ion exchange resins. J Hazard Mater 167:482–488. https://doi.org/10.1016/j.jhazmat.2009.01.006
10. Aysan H, Edebali S, Ozdemir C, Celik Karakaya M, Karakaya N (2016) Use of chabazite, a naturally abundant zeolite, for the investigation of the adsorption kinetics and mechanism of methylene blue dye. Micropor Mesopor Mater 235:78–86. https://doi.org/10.1016/j.micromeso.2016.08.007
11. Huang Q, Liu M, Chen J, Wan Q, Tian J, Huang L, Jiang R, Deng F, Wen Y, Zhang X, Wei Y (2017) Marrying the mussel inspired chemistry and Kabachnik–Fields reaction for preparation of SiO_2 polymer composites and enhancement removal of methylene

blue. Appl Surf Sci 422:17–27. https://doi.org/10.1016/j.apsusc.2016.06.037
12. Luo X-P, Fu S-Y, Du Y-M, Guo J-Z, Li B (2017) Adsorption of methylene blue and malachite green from aqueous solution by sulfonic acid group modified MIL-101. Micropor Mesopor Mater 237:268–274. https://doi.org/10.1016/j.arabjc.2018.07.004
13. Landaburu-Aguirre J, Pongrácz E, Sarpola A, Keiski LR (2012) Simultaneous removal of heavy metals from phosphorous rich real wastewaters by micellar-enhanced ultrafiltration. Sep Purif Technol 88:130–137. https://doi.org/10.1016/j.seppur.2011.12.025
14. Ali I (2012) New generation adsorbents for water treatment. Chem Rev 112:5073–5091. https://doi.org/10.1016/j.jenvman.2012.08.028
15. Martini BK, Daniel TG, Corazza MZ, de Carvalho AE (2018) Methyl orange and tartrazine yellow adsorption on activated carbon prepared from boiler residue: kinetics, isotherms, thermodynamics studies and material characterization. J Environ Chem Eng. https://doi.org/10.1016/j.jece.2018.10.013
16. Xiaoning W, Nanwen Z, Bingkui Y (2008) Preparation of sludge-based activated carbon and its application in dye wastewater treatment. J Hazard Mater 153:22–27
17. Ali I (2010) The quest for active carbon adsorbent substitutes: inexpensive adsorbents for toxic metal ions removal from wastewater. Purif Rev 39:95–171
18. Ali I, Asim M, Khan AT (2012) Low cost adsorbents for the removal of organic pollutants from wastewater. J Environ Manag 113:170–183
19. Ofomaja EA (2008) Kinetic study and sorption mechanism of methylene blue and methyl violet onto mansonia (mansonia altissima) wood sawdust. Chem Eng J 143:85–95. https://doi.org/10.1016/j.cej.2007.12.019
20. Sajab SM, Chia HC, Zachariah S, Jani SM, Ayob KM (2011) Citric acid modified knead core fibres for removal of methylene blue from aqueous solution. Bioresour Technol 102:7237–7243. https://doi.org/10.1016/j.biortech.2011.05.011
21. Hameed HB (2009) Removal of cationic dye from aqueous solution using jackfruit peel nonconventional low-cost adsorbent. J Hazard Mater 162:344–350. https://doi.org/10.1016/j.jhazmat.2008.05.045
22. Liu HJ, Zhang L, Zha CD, Chen QL, Chen XX, Qi MZ (2018) Biosorption of malachite green onto *Haematococcus pluvialis* observed through synchrotron-FTIR microspectroscopy. Lett Appl Microbiol. https://doi.org/10.1111/lam.13043
23. Han R, Zhang L, Song C, Zhang M, Zhu H, Zhang L (2010) Characterization of modified wheat straw, kinetic and equilibrium study about copper ion and methylene blue adsorption in batch mode. Carbohydr Polym 79:1140–1149. https://doi.org/10.1016/j.carbpol.2009.10.054
24. Svancara I, Vytras K, Kalcher K, Walcarius A, Wang J (2009) Carbon paste electrodes in facts, numbers, and notes: a review on the occasion of the 50-years jubilee of carbon paste in electrochemistry and electroanalysis. Electroanalysis 21:7–18. https://doi.org/10.1002/elan.200804340
25. Wang F, Zhang L, Wang Y, Liu X, Rohani S, Lu J (2017) Fe_3O_4@SiO_2@CS-TETA functionalized graphene oxide for the adsorption of methylene blue (MB) and Cu(II). Appl Surf Sci 420:970–981. https://doi.org/10.1016/j.apsusc.2017.05.179
26. Hui Y, Nan L, Shu X, Jin-Zhong X, Jun-Jie Z, Hong-Yuan C (2005) Electrochemical study of a new methylene blue/silicon oxide nanocomposition mediator and its application for stable biosensor of hydrogen peroxide. Biosens Bioelectron 21:372–377. https://doi.org/10.1016/j.bios.2004.08.051
27. Jun H, Hedayatollah G, Saeed ZR, Akbar MMA, Shahin A, Akbar SA (2007) Nafion-methylene blue functional membrane and its application in chemical and biosensing. Anal Lett 40:483–496. https://doi.org/10.1080/00032710601017664
28. Burcu M, Kagan K, Dilsat O, Pinar K, Selda E, Ulus AS, Marco M, Mehmet O (2002) Electrochemical DNA biosensor for the detection of TT and Hepatitis B virus from PCR amplified real samples by using methylene blue. Talanta 56:837–846. https://doi.org/10.1016/S0039-9140(01)00650-6
29. Ling Z, Ruijun Z, Kegang W, Haibo X, Zhimei S, Wei S (2008) Electrochemical behaviours of methylene blue on DNA modified electrode and its application to the detection of PCR product from NOS sequence. Sensors 8:5649–5660. https://doi.org/10.3390/s8095649
30. Tonle KI, Ngameni E, Tcheumi LH, Tchiéda V, Carteret C, Walcarius A (2008) Sorption of methylene blue on an organic clay bearing thiol groups and application to electrochemical sensing of the dye. Talanta 74:489–947. https://doi.org/10.1016/j.talanta.2007.06.006
31. Gong R, Feng M, Zhao J, Cai W, Liu L (2009) Functionalization of sawdust with monosodium glutamate for enhancing its malachite green removal capacity. Bioresour Technol 100:975–978. https://doi.org/10.1016/j.biortech.2008.06.060
32. Van Soest JP, Wine HR (1967) Use of detergents in the analysis of fibrous feeds. IV. Determination of plant cell wall constituents. J Am Oil Chem Soc 50:50–55
33. Van Soest JP, Wine HR (1968) Determination of lignin and cellulose in acid detergent fiber with permanganate. J Am Oil Chem Soc 51:780–784
34. Tonlé KI, Letaief S, Ngameni E, Walcarius A, Detellier C (2011) Square wave voltammetric determination of lead(II) ions using a carbon paste electrode modified by a thiol-functionalized kaolinite. Electroanalysis 23:245–252. https://doi.org/10.1002/elan.201000467
35. Nanseu-Njiki PC, Dedzo KG, Ngameni E (2010) Study of the removal of paraquat from aqueous solution by biosorption into Ayous (*Triplochiton schleroxylon*) sawdust. J Hazard Mater 179:63–71. https://doi.org/10.1016/j.jhazmat.2010.02.058
36. Mussatto IS, Carneiro ML, Silva APJ, Roberto IC, Teixeira JA (2011) A study on chemical constituents and sugars extraction from spent coffee grounds. Carbohydr Polym 83:368–374. https://doi.org/10.1016/j.carbpol.2010.07.063
37. El-Aziz A, Said A, Ludwick GA, Aglan HA (2009) Usefulness of raw bagasse for oil absorption a comparison of raw and acylated bagasse and their components. Bioresour Technol 100:2219–2222. https://doi.org/10.1016/j.biortech.2008.09.060
38. Le Digabel F, Averous L (2006) Effects of lignin content on the properties of lignocellulose-based bio composites. Carbohydr Polym 66:537–545. https://doi.org/10.1016/j.carbpol.2006.04.023
39. Murthy SP, Naidu MM (2012) Sustainable management of coffee industry by-products and value addition—a review. Resour Conserv Recycl 6:45–58. https://doi.org/10.1016/j.resconrec.2012.06.005
40. Mellah A, Chagrouche S (1997) The removal of zinc from aqueous solutions by natural bentonite. Water Resour 31:621–629. https://doi.org/10.3390/w10050621
41. Febrianto J, Kosasih AN, Sunarso J, Ju Y, Indraswati N, Ismadji S (2009) Equilibrium and kinetic studies in adsorption of heavy metals using biosorbent: a summary of recent studies. J Hazard Mater 162:616–645. https://doi.org/10.1016/j.jhazmat.2008.06.042
42. Rodriguez HM, Yperman J, Carleer R, Maggen J, Dadi D, Gryglewicz G, Van der Bruggen B, Hermandez FJ, Calvis OA (2018) Adsorption of Ni(II) on spent coffee and coffee husk based activated carbon. J Environ Chem Eng 6:1151–1170. https://doi.org/10.1016/j.jece.2017.12.045

43. Mahmoud AM (2015) Design of batch process for preconcentration and recovery of U(VI) from liquid waste by powdered corn cobs. J Environ Chem Eng. https://doi.org/10.1016/j.jece.2015.06.002
44. Nath S, Dutta PD (2018) Low cost synthesis of SiO_2/C nanocomposite from corn cobs and its adsorption of uranium (VI), chromium (VI) and cationic dyes from wastewater. J Mol Liq 269:140–151. https://doi.org/10.1016/j.moliq.2018.08.028
45. Duan XL, Yuan CG, Jing TT, Yuan XD (2019) Removal of elemental mercury using large surface area micro-porous corn cob activated carbon by zinc chloride activation. Fuel 239:830–840. https://doi.org/10.1016/j.fuel.2018.11.017
46. Aluigi A, Rombaldoni F, Tonetti C, Jannoke L (2014) Study of methylene blue adsorption on keratin nanofibrous membranes. J Hazard Mater 268:156–165. https://doi.org/10.1016/j.jhazmat.2014.01.012
47. Khelifi O, Nacef M, Affoune MA (2018) Nickel (II) adsorption from aqueous solutions by physio-chemically modified sewage sludge. Iran J Chem Chem Eng 37:73–87
48. Ariful Ahsan M, Islam TM, Imam AM, Hyder GA, Jabbari V, Dominguez N, Noveron CJ (2018) Biosorption of Bisphenol A and sulfamethoxazole from water using sulfonated coffee waste: isotherm, kinetic and thermodynamic studies. J Environ Chem Eng. https://doi.org/10.1016/j.jece.2018.10.004
49. McKay G, Mesdaghinia A, Nasseri S, Hadi M, Solaimany Aminabad M (2014) Optimum isotherms of dyes sorption by activated carbon: fractional theoretical capacity and error analysis. Chem Eng J 251:236–247. https://doi.org/10.1016/j.cej.2013.09.051
50. Guarín JR, Moreno-Piraján JC, Giraldo L (2018) Kinetic study of the bio adsorption of methylene blue on the surface of the biomass obtained from the algae *D. Antarctica*. J Chem. https://doi.org/10.1155/2018/2124845
51. Karim AB, Mounir B, Hachkar M, Bakasse M, Yaacoubi A (2009) Removal of basic Red 46 dye from aqueous solution by adsorption onto moroccan clay. J Hazard Mater 168:304–309. https://doi.org/10.1016/j.jhazmat.2009.02.028
52. Banat F, Al-Asheh S, Al-Ahmad R, Bni-Khalid F (2007) Bench scale and packed bed sorption of methylene blue using treated olive pomace and charcoal. Bioresour Technol 98:3017–3027
53. Zhu L, Zhang M, Xu L (2015) Removal of methylene blue dye from water by bagasse and corn cob. J Sci Technol 33:93–96. https://doi.org/10.1016/j.compscitech.2013.12.024
54. Conrad EK, Nnaemeka OJ, Chris AO (2015) Adsorptive removal of methylene blue from aqueous solution using agricultural waste: equilibrium, kinetic and thermodynamic studies. Am J Chem Mater Sci 2:14–25
55. Oliveira LS, Franca AS, Alves TM, Rocha SD (2008) Evaluation of untreated coffee husks as potential biosorbents for treatment of dye contaminated waters. J Hazard Mater 155:507–512. https://doi.org/10.1016/j.jhazmat.2007.11.093
56. Alshabanat M, Alsenani G, Almufarij R (2013) Removal of crystal violet dye from aqueous solutions onto date palm fibre by adsorption technique. J Chem 2013:1–6. https://doi.org/10.1155/2013/210239
57. Mbokou FS, Pontié M, Bouchara J-P, Tchieno MMF, Njanja É, Mogni A, Pontalier PY, Tonle KI (2016) Electro analytical performance of a carbon paste electrode modified by coffee husks for the quantification of acetaminophen in quality control of commercialized pharmaceutical tablets. Int J Electrochem. https://doi.org/10.1155/2016/1953278
58. Pontié M, Mbokou FS, Bouchara J-P, Razafimandimby B, Egloff S, Dzilingomo O, Pontalier P-Y, Tonle KI (2018) Paracetamol sensitive cellulose-based electrochemical sensors. J Renew Mater 6:242–250. https://doi.org/10.7569/JRM.2017.634169